IEEE Access
Multidisciplinary | Rapid Review | Open Access Journal

Received July 2, 2021, accepted August 1, 2021, date of publication August 5, 2021, date of current version August 16, 2021.

Digital Object Identifier 10.1109/ACCESS.2021.3102655

String Stability and Platoon Safety Analysis of a New Car-Following Model Considering a Stabilization Strategy

MINGFEI MU[1], JUNJIE ZHANG[2], CHANGMIAO WANG[3], JUN ZHANG[2], AND CAN YANG[2]

[1]College of Mechanical and Electronic Engineering, Shandong University of Science and Technology, Qingdao 266590, China
[2]Hefei Innovation Research Institute, Beihang University, Hefei 230012, China
[3]Shenzhen Research Institute of Big Data, Shenzhen 518115, China

Corresponding authors: Junjie Zhang (zhangjunjie55@163.com) and Changmiao Wang (wangcm@sribd.cn)

This work was supported in part by the National Key Research and Development Program of China under Grant 2018YFB1601100 and Grant 2018YFC0807500, in part by the Program of Hefei Science City of Beihang under Grant BHKX-21-06, in part by the Chinese Postdoctoral Science Foundation Science under Grant 2019M660407, in part by the National Natural Science Foundation of China under Grant 61802132, in part by the Guangdong Key Area Research and Development Fund with Project under Grant 2018B030338001, and in part by the Shandong Provincial Natural Science Foundation under Grant ZR2020QE164.

ABSTRACT Adaptive cruise control (ACC) systems can reduce collision risk and make traffic flow more smoothly; nevertheless, improving the string stability and car-following safety in ACC systems has remained an important research topic. Based on the desired safety margin (DSM) model adopted as an ACC velocity control method, a sliding mode controller is proposed to investigate string stability and car-following safety using the time headway policy (THP), and its stability is verified by the Lyapunov stability theory. Furthermore, numerical simulations are conducted to verify the effectiveness of the proposed stabilization strategy for the stability of the DSM model. Analyzing the risk assessment indexes (time-to-collision, TTC, and time headway, TH) of the DSM model reveals that the proposed stabilization strategy can improve the traffic flow stability and avoid rear-end collision risks when the leading car exhibits a small disturbance. Therefore, the proposed stabilization strategy is valuable for designing ACC controllers to enhance traffic flow stability and car-following safety in automotive platoon driving.

INDEX TERMS String stability, safety margin, adaptive cruise control system, stabilization strategy, time headway policy.

I. INTRODUCTION

Traffic congestion and safety problems have been increasingly threatening environmental and economic development in modern society. Humans play a key role in transportation systems because they are the participants, handlers, controllers, and decision makers of all driving behaviors that significantly influence roadway performance and traffic safety [1], [2]. Thus, traffic flow stability and the reduction in collision risk should be improved. Intelligent transportation systems (ITSs) and vehicle-to-vehicle (V2V) communication can detect potential risk situations, thereby avoiding collisions and improving vehicle control performance [3]. Therefore, problems with adaptive cruise control (ACC) systems and controlling vehicle formations have attracted extensive attention.

Recently, ACC systems have been widely installed in vehicles to improve string stability and platoon (car-following) safety [4]–[6], and the system mainly comprises information collection equipment, vehicle longitudinal dynamic models (one of the core parts), and human machine interactive systems. In terms of modeling, complete communications between vehicles were taken into account to build a mass spring damper system [7]. Franck *et al.* [8] believed that vehicle interactions are based on physical phenomena or mimic animal interaction behaviors when a vehicular platoon is considered a multiagent system. Yi and Chong [9] deemed that interactions are considered virtual spring damper systems. The nonlinear longitudinal dynamic model was proposed by Lu *et al.* [10], and includes road resistance, gravity,

The associate editor coordinating the review of this manuscript and approving it for publication was Shajulin Benedict.

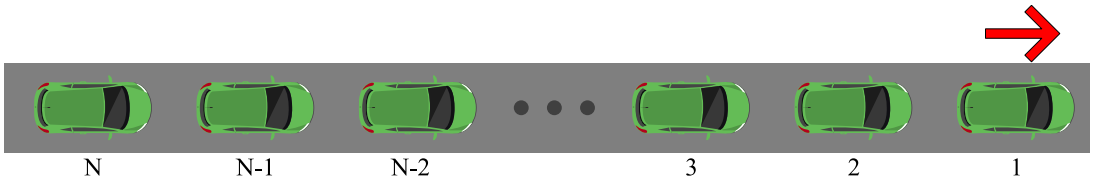

FIGURE 1. A platoon of *N* vehicles.

aerodynamic drag, and other influencing factors. Zheng *et al.* [11] used some state variables, such as position, speed, and acceleration/deceleration, to build a linearized vehicle longitudinal dynamic model. Later, Milanes *et al.* [12] built a second-order response model with time delay to characterize a vehicle longitudinal model during the starting and braking process on the basis of experimental test data. In addition, the intelligent driver model (IDM) [13], [14] and its extended models [15], [16] can be well applied to the vehicle longitudinal dynamic model of ACC vehicles to analyze the effect of different ACC strategies on traffic flow. Kerner [17], [18] proposed a three-traffic-phase ACC (TPACC) model and found that the TPACC approach can result in more merits (i.e., ensuring string stability, decreasing the probability of traffic flow breakdown and velocity disturbances) than the classical approach to ACC. Likewise, Lu *et al.* [19], [20] clarified car-following behaviors by defining a safety margin, and proposed a desired safety margin (DSM) model. and geographic information system is also applied on the study of driving behavior. Although the aforementioned vehicle longitudinal dynamic models have a good ability to simulate the whole car-following processes of ACC vehicles, how to improve the ACC vehicle platoon stability is still a matter of concern for scholars. That is, the basic requirement of applying ACC to vehicles is performance stability, which ensures the comfortableness and safety of drivers and passengers in platooning applications [21]. Therefore, string stability, which is a key property of platoon control, has attracted the attention of scholars [22].

The string stability indicates that the spacing headway error, states, or the control input are not amplified as a small perturbation propagation upstream from one vehicle to another vehicle in the platoons. Several control strategies have been introduced in vehicle platoons to improve string stability [23], [24]. In general, two major car-following spacing policies (constant spacing policy, CSP; constant time headway policy, CTHP), have been used to reduce the propagation of disturbances in platoons. Between these policies, a CSP is usually applied because it not only enhances string stability but also achieves high traffic capacity [25]–[31]. However, this policy is founded on a realistic assumption of the initial speed and zero spacing error and requires the cost of vehicle-to-vehicle communications [30]. The CTHP is a simple and common variable spacing policy [32]. This policy can enhance string stability using onboard information. Thus, the CTHP is typically adopted to replace the CSP for controlling vehicle platoons [33]–[39]. Compared with the CSP, steady-state intervehicle spacing can be enlarged with increasing velocity, which leads to a low traffic density [34]. Swaroop *et al.* [40] presented a comparative study of time headway policy and spacing for automatic control vehicles, and the results show that spacing control is a very attractive method without requiring intervehicle communication for autonomous intelligent cruise control systems. Recently, Ali *et al.* [41] modified the CTHP and improved string stability by introducing a virtual truck. However, this policy increases the risk of collision due to the small distances between vehicles. Guo *et al.* [42] presented a distributed adaptive sliding mode control strategy that is based on the modified CTHP to improve the string stability.

According to these studies, string stability is strongly correlated to the control strategy of vehicle platoons, which is significant in the theory and practice of ACC systems.

ACC systems are longitudinal driving assistant systems that can detect and identify leading vehicles and maintain space headways by constantly adjusting a vehicle's speed on the basis of a control algorithm. Most dynamic models of ACC vehicles are car-following model-based ACC models, including the IDM and its extended models, the extended OV model, the state variable-based linearized vehicle longitudinal dynamic model, etc. However, most dynamic models cannot simulate different drivers' physiological and psychological characteristics. That is, most ACC systems require drivers to adjust their behavior to adapt to these systems. Satisfying the requirements of drivers' individual comfort in this manner is difficult because different drivers have varying driving habits. In contrast, the vehicle dynamic model based on the risk measure of the DSM is capable of detecting drivers' physiological and psychological characteristics using five driving behavior parameters.

In this study, the DSM model is used to develop a corresponding dynamic control scheme, investigate string stability, and verify the effectiveness of our proposed stabilization strategy. The findings will promote the development of the DSM model in ACC systems.

II. DSM CAR-FOLLOWING MODEL

We consider that a platoon of N vehicles run on a straight road as shown in Figure 1. All vehicles follow their preceding vehicle based on the DSM car-following model [20]. The acceleration of the nth follower vehicle can be written as

$$a_n(t+\tau) = \begin{cases} \alpha_1 \left(VM_n(t) - VM_{nDH}\right), & VM_n(t) > VM_{nDH} \\ \alpha_2 \left(VM_n(t) - VM_{nDL}\right), & VM_n(t) < VM_{nDL} \\ 0, & else \end{cases} \tag{1}$$

where α_1 is the sensitivity factor for acceleration, α_2 is the sensitivity factor for deceleration $a_n(t)$ is the acceleration of the nth vehicle at time t, VM_{nDH} is the upper limit of the DSM, VM_{nDL} is the lower limit of the DSM, and $VM_n(t)$ is the value of the DSM.

And

$$VM_n(t) = 1 - \frac{v_n(t)\cdot\tau_b + \left([v_n(t)]^2/2d_n(t)\right)}{x_{n-1}(t) - x_n(t) - l_{n-1}} + \frac{[v_{n-1}(t)]^2/2d_{n-1}(t)}{x_{n-1}(t) - x_n(t) - l_{n-1}} \quad (2)$$

where $v_n(t)$ is the velocity of the nth vehicle at time t, $x_n(t)$ is the position of the nth vehicle at time t, l_{n-1} is the length of the $(n-1)$th vehicle, $d_n(t)$ is the deceleration of the nth vehicle at time t, τ is the reaction time, and τ_b is the brake system's reaction time.

The DSM model can be used as the control strategy of the ACC system [43], VM_{nDL} and VM_{nDH} denote the acceptable gaps between two successive vehicles with the ACC system in the platoon, τ can denote the response time of vehicles with the ACC system, and α_1 and α_2 denote the acceleration and deceleration response characteristics of vehicles within the ACC system.

Several supplementary constraints are imposed to satisfy the limitations in the vehicle motion in the car-following process as follows.

(1) Maximum deceleration: a vehicle's deceleration ranges from approximately 2 m/s^2 to 8 m/s^2 on the basis of the Highway Capacity Manual [44]. Therefore, the maximum deceleration of vehicles with the ACC system is set to less than -8 m/s^2.

(2) Maximum favorite acceleration: a vehicle's acceleration ranges from approximately 0.9 m/s^2 to 4 m/s^2 on the basis of the Highway Capacity Manual [44]. In addition, Treiber *et al.* declared that a vehicle's acceleration ranges from approximately 0.8 m/s^2 to 2.5 m/s^2 [45]. However, the maximum favorite acceleration is set as 1.5 m/s^2 in the Gipps car-following model [46]. Therefore, the maximum favorite acceleration is set as 1.5 m/s^2; that is $a_n(t) = 1.5$ m/s^2 if $a_n(t) > 1.5$ m/s^2.

(3) Minimum relative spacing headway: Lu *et al.* [20] estimated a relatively acceptable spacing headway for drivers in the car-following process, found that the relative acceptable spacing headway ranges from approximately 1.07 m to 4.83 m, and its median is 1.90 m. Therefore, the minimum relative spacing headway constraints were set as

$$a_n(t) = \max\left\{\frac{-[v_n(t)]^2}{(2\cdot\max[(\Delta x_n(t) - l_{n-1} - S_0), 0.01])}, -8.0\text{m}/s^2\right\},$$

in which S_0 is the minimum favorite gap when two vehicles are at a stop and is set to 1.9 m. $\max[(\Delta x_n(t) - l_{n-1} - S_0), 0.01]$ can be used to avoid $[v_n(t)]^2/(2\cdot\max[(\Delta x_n(t) - l_{n-1} - S_0), 0.01])$, which is unreasonable.

Lu *et al.* [20] used the vector $P = (\tau, VM_{nDL}, VM_{nDH}, \alpha_1, \alpha_2)^T$ to describe the car-following behaviors of different drivers. In the ACC system, the control parameters of the DSM model are set to $\tau = 0.5 VM_{nDL} = 0.75$, $VM_{nDH} = 0.94$, $\alpha_1 = 6.43$, and $\alpha_2 = 12.22$. In addition, other parameters of the DSM model, such as $d_n(t) = 7.35$ and $d_{n-1}(t) = 7.35$[47], $\tau_b = 0.15$ s because its value remains within the limits of 0.1 to 0.2 s for most Japanese and Western vehicles in emergency situations [48].

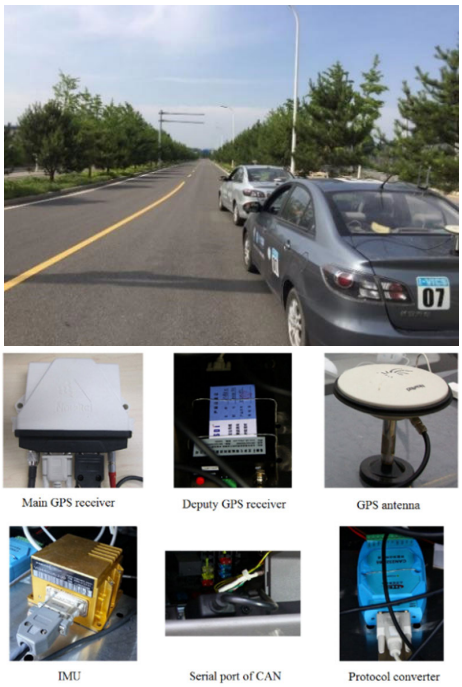

FIGURE 2. Two test vehicles, GPSs, IMU and other components of the ACC system.

Furthermore, two test vehicles with a speed control system (DSM model) are used to collect experimental data in Tian Gong Road, as shown in Figure 2.

Based on the test results of the car-following performance, fluctuations between the detected headway and the desired headway were detected, as shown in Figure 3, in which the velocity difference between the leading vehicle and the following vehicle was more than ±2 m/s when the velocity of the leading vehicle slightly fluctuated [49]. As suggested in Wagner [50] and Jiang *et al.* [51], if the fluctuation is approximately ±2 m/s, then the headways of all vehicles in the platoon have large fluctuations. This result implies that unstable traffic flow may occur [52] with a small disturbance of the leading vehicle acceleration in the platoon. Therefore, the results show that the DSM control strategy should be improved to enhance string stability and car-following safety. How to further improve the DSM model stability is a problem worth studying.

III. PLATOON CONTROL SCHEME

A. NOTATIONS

Symbol	Quantity
S	desired spacing headway
e_n	spacing error

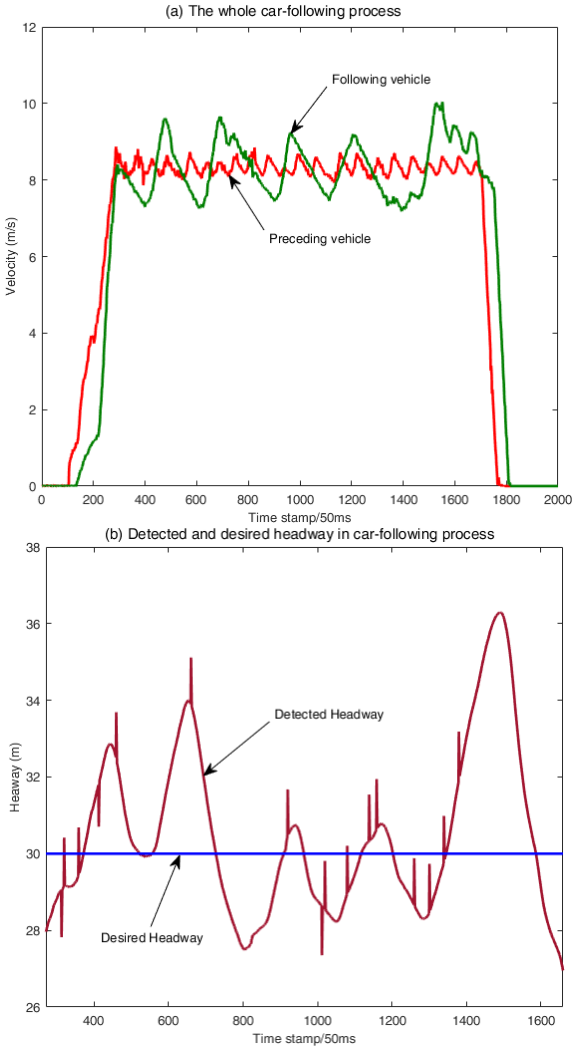

FIGURE 3. The whole car-following processes in the DSM model.

x_{n-1}	position of the (n-1) th vehicle
x_n	position of the n th vehicle
δ_n	new spacing error
H	time headway between the (n-1) th and n th vehicles
v^*	same velocity for all vehicles in a stable platoon
Δx^*	same space headway for all vehicles in a stable platoon
χ_{DSM}	feasible value between the lower and the upper limits of the DSM
s_n	gap between the n th vehicle and the (n-1) th vehicle
εv_n	small perturbation of the velocity around the steady-state solution
εs_n	small perturbation of the gap around the steady-state solution
$u_n^i(t)$	control signal term
Θ_0	new gap error
k_1, ρ, γ	positive constants

B. SLIDING MODE CONTROLLER STABILITY ANALYSIS

In this study, the vehicle platoon comprises many equipped vehicles following one another, and each vehicle can receive the motion information of its preceding vehicle. Other vehicles follow one another, moving at the same velocity $V(S)$ and with the same desired spacing headway S, and the 1st vehicle is the leading car, as shown in Figure 4.

Then, the spacing headway error e_n of the nth vehicle can be defined as follows:

$$e_n = x_{n-1} - x_n - S. \tag{3}$$

As suggested in [41], the kinematic evolution can be defined as follows:

$$\dot{e_n} = \dot{x_{n-1}} - \dot{x_n}. \tag{4}$$

The dot above e_n denotes the differentiation regarding the time.

Therefore, the goal of the control strategy is $\lim_{t \to t_0} e_n = 0$ in the constant spacing control, and t_0 is a constant ($t_0 > 0$). However, the nth vehicle's new spacing error δ_n is defined in the time headway policy as follows:

$$\delta_n = e_n - Hv_n. \tag{5}$$

Similarly, this control strategy drives δ_n to 0. Previous studies have shown that the THP eliminates the requirement of communication with the leading vehicle and increases the intervehicle distance with velocity. This condition implies that the THP is superior to a constant spacing control strategy. Equation (2) can be written by the DSM as follows:

$$0 = \alpha_1 \left(\begin{array}{l} 1 - \dfrac{2d_n(t) \cdot v_n(t) \cdot \tau_b + [v_n(t)]^2}{2d_n(t)\,[x_{n-1}(t) - x_n(t) - l_{n-1}]} \\ + \dfrac{[v_{n-1}(t)]^2}{2d_{n-1}(t)\,[x_{n-1}(t) - x_n(t) - l_{n-1}]} - VM_{nDH} \end{array} \right) \tag{6}$$

and

$$0 = \alpha_2 \left(\begin{array}{l} 1 - \dfrac{2d_n(t) \cdot v_n(t) \cdot \tau_b + [v_n(t)]^2}{2d_n(t)\,[x_{n-1}(t) - x_n(t) - l_{n-1}]} \\ + \dfrac{[v_{n-1}(t)]^2}{2d_{n-1}(t)\,[x_{n-1}(t) - x_n(t) - l_{n-1}]} - VM_{nDL} \end{array} \right) \tag{7}$$

H can be calculated as follows:

$$H = \frac{\tau_b}{1 - \chi_{DSM}} + \frac{l}{v^*}. \tag{8}$$

where $\chi_{DSM} = \langle VM_{nDL}, VM_{nDH} \rangle$, $v_n = v_{n-1} = v^*$, $d_n = d_{n-1}$, and $l_{n-1} = l$.

For the convenience of qualitative analysis, the DSM model can be written as follows:

$$\begin{cases} \dfrac{dv_n(t)}{dt} = f_i(v_{n-1}, s_n, v_n), \\ \dfrac{ds_n(t)}{dt} = v_{n-1}(t) - v_n(t). \end{cases} \tag{9}$$

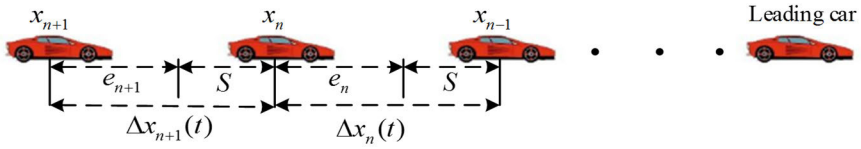

FIGURE 4. Vehicle platoon.

where the function $f_i(v_{n-1}, s_n, v_n) = \alpha_i (VM_n(t) - VM_{nDH})$, $i = 1, 2$.

Specifically, the velocity of the considered vehicle is given by $v_n = v_{n-1} = \cdots = v^*$, and the gap of the considered vehicle is given by $s_n = s_{n-1} = \cdots = s^*$, which satisfies the function $f(v^*, s^*, v^*) = 0$. We define $v_n = v^* + \varepsilon v_n$ and $s_n = s^* + \varepsilon s_n$, respectively. Then, Equation (10) can be written as

$$\begin{cases} \dfrac{d\varepsilon v_n(t)}{dt} = f_i^{v_{n-1}} \varepsilon v_{n-1}(t) + f_i^{s_n} \varepsilon s_n(t) + f_i^{v_n} \varepsilon v_n(t), \\ \dfrac{d\varepsilon s_n(t)}{dt} = \varepsilon v_{n-1}(t) - \varepsilon v_n(t). \end{cases} \tag{10}$$

where

$$\begin{aligned} f_i^{v_n} &= \left.\frac{\partial f}{\partial v_n}\right|_{(v^*,s^*)} = -\alpha_i \frac{\tau_b d + v^*}{s^* d}, \\ f_i^{s_n} &= \left.\frac{\partial f}{\partial s_n}\right|_{(v^*,s^*)} = \alpha_i \frac{v^* \tau_b}{(s^*)^2}, \\ f_i^{v_{n-1}} &= \left.\frac{\partial f}{\partial v_{n-1}}\right|_{(v^*,s^*)} = \alpha_i \frac{v^*}{s^* d}. \end{aligned} \tag{11}$$

where $d_n = d_{n-1} = d$.

A control signal term $u_n^i(t)$ is added, and Equation (10) can be written as follows:

$$\begin{cases} \dfrac{d\varepsilon v_n(t)}{dt} = f_i^{v_{n-1}} \varepsilon v_{n-1}(t) + f_i^{s_n} \varepsilon s_n(t) + f_i^{v_n} \varepsilon v_n(t) + u_n^i(t), \\ \dfrac{d\varepsilon s_n(t)}{dt} = \varepsilon v_{n-1}(t) - \varepsilon v_n(t). \end{cases} \tag{12}$$

Furthermore, the new gap error Θ_0 can be defined on the basis of Equations (6) and (9) as follows:

$$\Theta_0 = \varepsilon s_n - \left(\frac{\tau_b}{1 - \chi_{DSM}} + \frac{l}{v^*}\right) \cdot \varepsilon v_n + l. \tag{13}$$

Then, the goal of the control scheme is $\lim_{t \to t_0} \Theta_0 = 0$.

A sliding mode controller of the vehicle platoon is brought in, in which the sliding mode surface is given as follows:

$$\Theta = \Theta_0 + k_1 \int_0^t \Theta_0 d\zeta. \tag{14}$$

Then,

$$\begin{aligned} \dot{\Theta} &= \dot{\Theta}_0 + k_1 \Theta_0 \\ &= \varepsilon v_{n-1}(t) - \varepsilon v_n(t) - \left(\frac{\tau_b}{1 - \chi_{DSM}} + \frac{l}{v^*}\right) \varepsilon \dot{v}_n(t) \\ &\quad + k_1 \left(\varepsilon S_n(t) - \left(\frac{\tau_b}{1 - \chi_{DSM}} + \frac{l}{v^*}\right) \varepsilon v_n(t) + l\right) \\ &= \left(1 - \frac{\alpha_i v^*}{s^* d}\left(\frac{\tau_b}{1 - \chi_{DSM}} + \frac{l}{v^*}\right)\right) \varepsilon v_{n-1}(t) \\ &\quad - \left(1 + k_1 \left(\frac{\tau_b}{1 - \chi_{DSM}} + \frac{l}{v^*}\right) - \alpha_i \frac{\tau_b d + v^*}{s^* d}\right) \varepsilon v_n(t) \\ &\quad + \left(k_1 - \frac{\alpha_i v^* \tau_b}{(s^*)^2}\left(\frac{\tau_b}{1 - \chi_{DSM}} + \frac{l}{v^*}\right)\right) \cdot \varepsilon S_n + k_1 l \\ &\quad - \left(\frac{\tau_b}{1 - \chi_{DSM}} + \frac{l}{v^*}\right) \cdot u_n^i(t) \end{aligned} \tag{15}$$

The candidate Lyapunov function is given as follows [53]–[55]:

$$\Sigma = \frac{1}{2}\Theta^2. \tag{16}$$

We obtain

$$\begin{aligned} \dot{\Sigma} &= \Theta\dot{\Theta} \\ &= \Theta \cdot \left[\begin{array}{l} \left(1 - \dfrac{\alpha_i v^*}{s^* d}\left(\dfrac{\tau_b}{1 - \chi_{DSM}} + \dfrac{l}{v^*}\right)\right) \varepsilon v_{n-1}(t) \\ - \left(1 + k_1 \left(\dfrac{\tau_b}{1 - \chi_{DSM}} + \dfrac{l}{v^*}\right) - \alpha_i \dfrac{\tau_b d + v^*}{s^* d}\right) \\ \varepsilon v_n(t) + \left(k_1 - \dfrac{\alpha_i v^* \tau_b}{(s^*)^2}\left(\dfrac{\tau_b}{1 - \chi_{DSM}} + \dfrac{l}{v^*}\right)\right) \\ \cdot \varepsilon s_n + k_1 l - \left(\dfrac{\tau_b}{1 - \chi_{DSM}} + \dfrac{l}{v^*}\right) \cdot u_n^i(t) \end{array}\right] \end{aligned} \tag{17}$$

Then, the sliding mode controller can be designed on the basis of (18) as follows:

$$\begin{aligned} & u_n^i(t) \\ &= \left(\frac{1}{\left(\frac{\tau_b}{1 - \chi_{DSM}} + \frac{l}{v^*}\right)} - \frac{\alpha_i v^*}{s^* d}\right) \varepsilon v_{n-1}(t) \\ &\quad - \left(k_1 + \frac{1 - \alpha_i \frac{\tau_2 d + v^*}{s^* d}}{\left(\frac{\tau_b}{1 - \chi_{DSM}} + \frac{l}{v^*}\right)}\right) \varepsilon v_n(t) \\ &\quad + \left(\frac{k_1}{\left(\frac{\tau_b}{1 - \chi_{DSM}} + \frac{l}{v^*}\right)} - \frac{\alpha_i v^* \tau_b}{(s^*)^2}\right) \cdot \varepsilon s_n \\ &\quad + \frac{k_1 l}{\left(\frac{\tau_b}{1 - \chi_{DSM}} + \frac{l}{v^*}\right)} + \frac{1}{\left(\frac{\tau_b}{1 - \chi_{DSM}} + \frac{l}{v^*}\right)} (\rho\Theta + \gamma \mathrm{sgn}(\Theta)). \end{aligned} \tag{18}$$

By substituting (19) into (18), we obtain

$$\dot{\Sigma} = \Theta\dot{\Theta} = \Theta(-\rho\Theta - \gamma \mathrm{sgn}(\Theta)) = -\rho\Theta^2 - \gamma |\Theta| \leq 0. \tag{19}$$

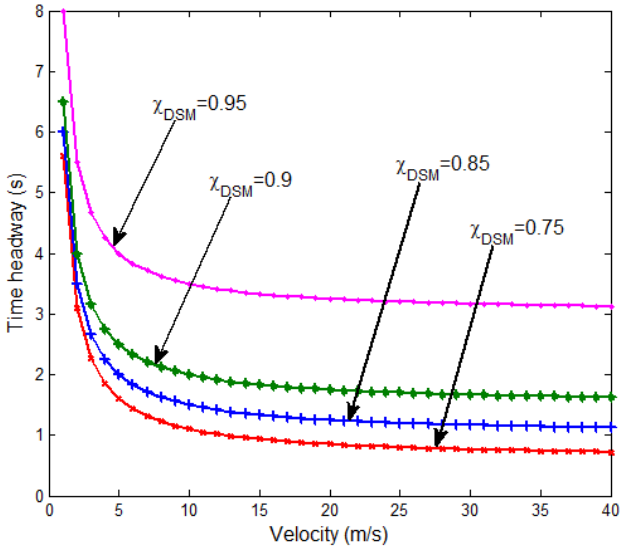

FIGURE 5. Relationship between *TH* and χ_{DSM} with $v^* = 20$ m/s.

Consequently, according to Lyapunov stability theory, the proposed sliding mode controller is stable.

Furthermore, Σ is a nonincreasing function because $\dot{\Sigma} \leq 0, t \in [0, +\infty)$. Thus, we obtain $\Sigma(t) \leq \Sigma(0) < \Sigma(+\infty)$. Since $\ddot{\Sigma} = \dot{\Theta}\dot{\Theta} + \Theta\ddot{\Theta} = -2\rho\Theta\dot{\Theta} - \gamma\dot{\Theta}|\Theta|$, we determine that $\Theta_0(t)$ and $\Theta(t)$ are bounded when $t \geq 0$. Since $\dot{\Theta}_0 = \varepsilon v_{n-1}(t) - \varepsilon v_n(t) - \left(\frac{\tau_b}{1-\chi_{DSM}} + \frac{l}{v^*}\right) \cdot \varepsilon \dot{v}_n(t)$, we determine that $\dot{\Theta}_0 \in L^\infty$. Moreover, we determine that $\dot{\Sigma}$ is uniformly continuous because $\ddot{\Sigma} \in L^\infty$.

In addition, when $\int_0^{+\infty} \left|\dot{\Sigma}\right| dt = |\Sigma(+\infty)| - |\Sigma(0)| < +\infty$, we have that $\lim_{t\to\infty} \int_0^t \left|\dot{\Sigma}(\zeta)\right| d\zeta$ is in existence and bounded. Based on Barbalat's lemma [56], if $\dot{\Sigma}$ is uniformly continuous and $\lim_{t\to\infty} \int_0^t \left|\dot{\Sigma}(\tau)\right| d\tau$ exists and is bounded, then $\lim_{t\to\infty} \dot{\Sigma} = 0$. Moreover, we know that $\dot{\Sigma} = \Theta(-\rho\Theta - \gamma \text{sgn}(\Theta)) \leq 0$. Then, we have $\lim_{x\to\infty} \left(\rho\Theta^2 + \gamma|\Theta|\right) = 0$. Therefore, we find that Θ and Θ_0 asymptotically converge to zero.

Moreover, a feasible χ_{DSM} should be given for the control term. According to Equation (9), there is a corresponding relation between χ_{DSM} and the time headway (*TH*). The *TH* should be higher than 2 s on the basis of several driving experiments in the US. Likewise, European nations recommended drivers to keep the time headway above 2 s [57]. Specifically, the average *TH* value for all subjects on road A35 was approximately 2 s. The relationship between the *TH* and χ_{DSM} is shown in Figure 5. The result shows that the average DSM was approximately 0.9 when the *TH* was 2 s [52]. Additionally, Lu *et al.* [19] found that the average of χ_{DSM} was approximately 0.9 for general drivers based on the experimental results of a real vehicle test. To meet the psychological characteristics of people in the car-following process, 0.9 was used to set the value of χ_{DSM}. Other control parameters were set as follows in the numerical simulation: $k_1 = 0.4$, $\rho = 0.01$, and $\gamma = 0.04$.

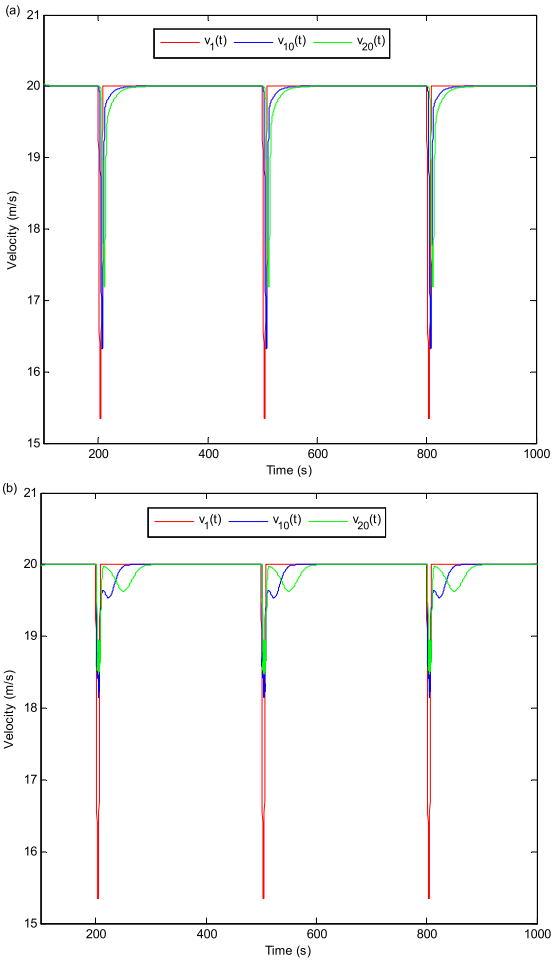

FIGURE 6. Velocity characteristics of the 1st, 10th and 20th vehicles: (a) without the stabilization strategy and (b) with our proposed stabilization strategy.

IV. NUMERICAL EXPERIMENTS AND DISCUSSION

The influence of the proposed stabilization strategy on the stability and safety of a platoon in the car-following process is studied through numerical experiments.

All vehicles' positions and speeds in the platoon vary with the time step $\Delta t = 0.1$ s, as shown in below:

$$v_n(t + \Delta t) = v_n(t) + \Delta t \cdot \dot{v}_n(t), \tag{20}$$

$$x_n(t + \Delta t) = x_n(t) + \Delta t \cdot \dot{x}_n(t) + \frac{1}{2}\ddot{x}_n(t) \cdot (\Delta t)^2. \tag{21}$$

Consider a case where 20 vehicles with a spacing headway $L = 35$ m move in a single lane. The following initial conditions are set for all vehicles:

$$\begin{aligned} x_{n-1}(0) &= L \cdot (N - n + 2), \\ v_{n-1}(0) &= 20, \\ \dot{v}_{n-1}(0) &= 0, \\ n &= 2, \cdots, N + 1. \end{aligned} \tag{22}$$

where $x_{n-1}(0)$ is the initial position of the $(n-1)$th vehicle in the system when $t = 0$, $v_{n-1}(0)$ is the initial velocity

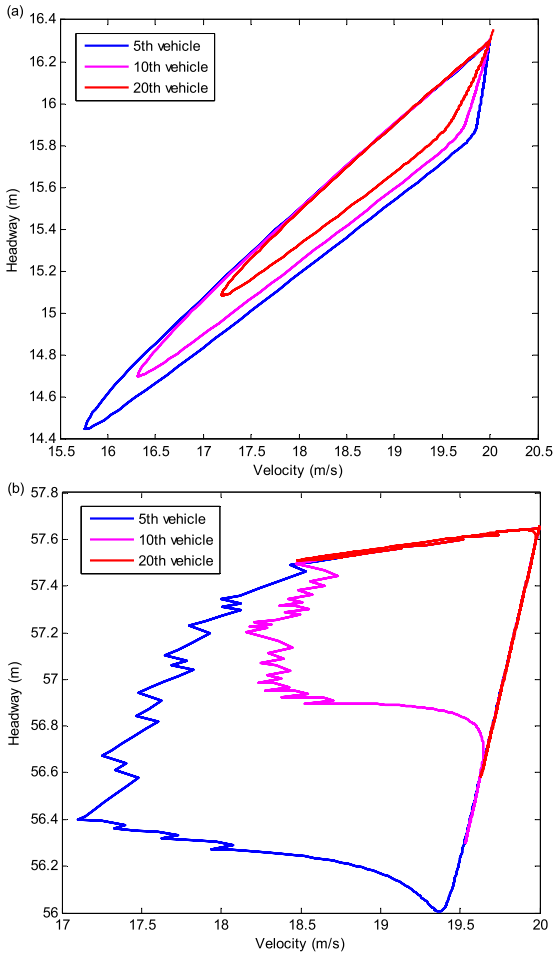

FIGURE 7. Hysteresis loops are obtained from the 5th, 10th, and 20th vehicles: (a) without the stabilization strategy and (b) with our proposed stabilization strategy.

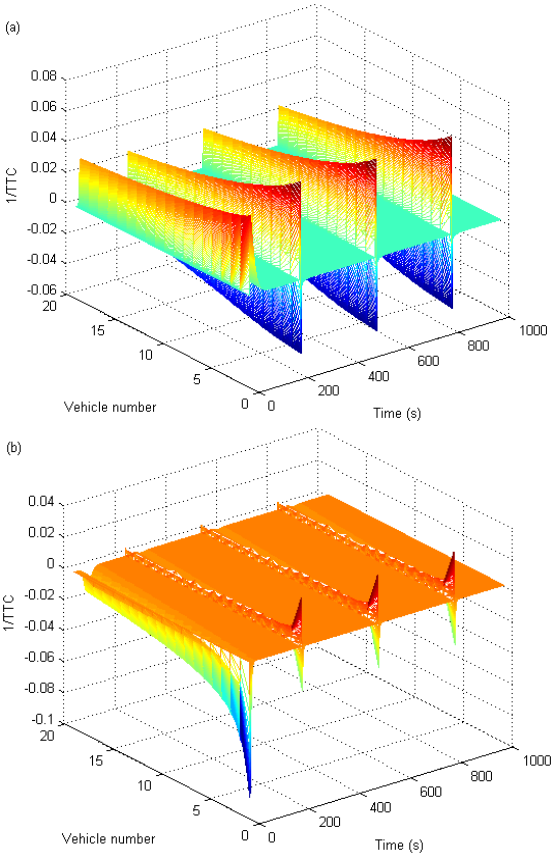

FIGURE 8. Spatiotemporal plot of the 1/*TTC* values of vehicles based on the DSM model: (a) without the stabilization strategy and (b) with our proposed stabilization strategy.

of the same vehicle when $t = 0$, and $\dot{v}_{n-1}(0)$ is the initial acceleration of the same vehicle when $t = 0$.

The traffic scene is established as follows: the first vehicle of the platoon abruptly decelerates at –1.5 m/s^2 during three short time intervals, namely, 200 to 203 s, 500 to 503 s, and 800 to 803 s, and the first vehicle of the platoon accelerates at 1.5 m/s^2 during three intervals, namely, 205 to 208 s, 505 to 508 s, and 805 to 808 s. These external disturbances are introduced to investigate the influence of our proposed stabilization strategy on the traffic safety and string stability.

Figure 6 illustrates the velocity characteristics of the 1st, 10th, and 20th vehicles in the DSM model with and without our proposed stabilization strategy after 100 s. The deviations in the speeds of the vehicles from the desired velocity of 20 m/s are reduced to a reasonable range of less than 2 m/s, as shown in Figure 6(b). Compared with Figure 6(a), the velocity fluctuations are effectively reduced under our proposed stabilization strategy.

Moreover, based on the DSM model, the hysteresis loops of the 5th, 10th, and 20th vehicles are obtained, as shown in Figure 7(a). Figure 7(b) illustrates that the hysteresis loops of the 5th, 10th, and 20th vehicles are obtained on the basis of the DSM model with our proposed stabilization strategy. The fluctuation in the hysteresis loops of the 5th, 10th, and 20th vehicles is smaller in the DSM model with our proposed stabilization strategy than in the DSM model without our proposed stabilization strategy. In addition, the platoon shows a larger spacing headway under the proposed ACC model, which verifies the relevant results of previous studies (i.e., steady-state intervehicle spacing of the time headway policy can be enlarged, and thus, the rear-end collisions would be reduced). Specifically, the hysteresis loops of the vehicles demonstrate that the string stability considering the proposed stabilization strategy is better than that not in the ACC system. Thus, the results show that our proposed stabilization strategy can effectively enhance the string stability.

In addition, Figure 7 shows that the headways of the vehicles are higher with the proposed stabilization strategy than those in the DSM model. This finding implies that our proposed stabilization strategy can improve car-following safety. The time-to-collision (*TTC*) and *TH* are two typical rear-end collision risk assessment indexes [22], and *TTC* is the remaining time until a collision occurs when two cars drive on the same route. However, risks are underestimated at large relative velocities as the influence of the relative velocity is ignored when calculating the *TH*. Therefore, the *TTC* should be selected as a risk measure index, and can be

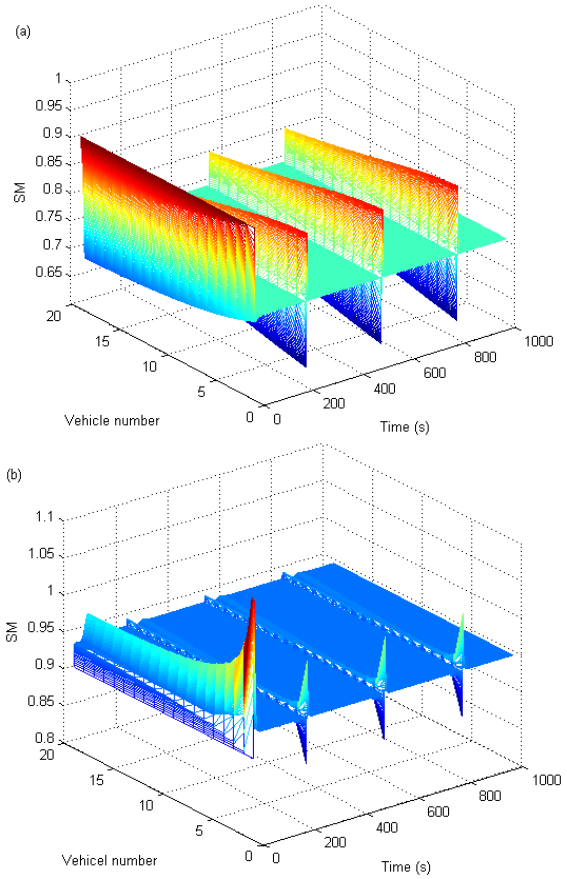

FIGURE 9. Spatiotemporal plot of the *SM* of vehicles based on the DSM model: (a) without the stabilization strategy and (b) with our proposed stabilization strategy.

calculated as follows:

$$TTC_n = \frac{\Delta x_n(t) - l_{n-1}}{v_n(t) - v_{n-1}(t)}, \quad \forall v_n(t) > v_{n-1}(t) \tag{23}$$

A large or an undefined *TTC* value may occur according to (23) when $v_n(t)$ and $v_{n-1}(t)$ are nearly equal in the platoon. Therefore, 1/*TTC* is adopted to represent the *TTC*.

Furthermore, the safety margin (*SM*), a new risk indicator, is adopted to evaluate the rear-end collision risk based on (3), and can be simplified as follows:

$$SM_n = 1 - \frac{1.5g \cdot 0.15 \cdot v_n(t) + [v_n(t)]^2}{1.5g\,[\Delta x_n(t) - l_{n-1}]} + \frac{[v_{n-1}(t)]^2}{1.5g\,[\Delta x_n(t) - l_{n-1}]} \tag{24}$$

Figure 8 illustrates that the spatiotemporal plot of 1/*TTC*, which is based on the DSM model, is obtained from all vehicles without and with the proposed stabilization strategy. As shown in Figure 8(a) and Figure 8(b), the 1/*TTC* of all vehicles increases from 0 to 0.02 with the external disturbance, whereas the 1/*TTC* also tends to zero. The fluctuation in 1/*TTC* with our proposed stabilization strategy is decreasing, compared to the 1/*TTC* without our proposed stabilization strategy.

Under the *SM* indicator, Figure 9(a) shows that the *SM* of all vehicles fluctuates between 0.6 and 0.9 and that all vehicles run orderly with $SM = 0.7$ when the external disturbance disappears. The *SMs* of all vehicles are in the range of 0.8 to 1, and the running *SM* of all vehicles obtains a high value with $SM = 0.95$, as shown in Figure 9(b). Therefore, collision risks with a small *SM* or *TTC* are observed. The results indicate that the proposed stabilization strategy can improve the traffic safety in the ACC system.

V. CONCLUSION

In this study, the DSM model was used as an ACC control strategy for a rear-end avoidance system. Thus, vehicles can adjust to a suitable velocity in the car-following process based on the proposed DSM-ACC system. This study analyses string stability and platoon safety based on the DSM car-following model considering a stabilization strategy. Specifically, the stability of the proposed sliding mode controller based on the time headway policy is guaranteed by using Lyapunov stability theory.

The numerical simulations demonstrate that the proposed stabilization strategy improves the smoothness of vehicular traffic flow and avoids a collision risk by using the *TTC* and *SM* indicators. The proposed theoretical analysis and strategy have provided an effective way to improve the string stability and safety of automotive platoon driving, which can be valuable when designing ACC controllers. Moreover, the DSM model as an ACC control strategy can satisfy the drivers' individual requirements. This research promotes the development of the DSM model in ACC or automotive driving platoons.

However, we have investigated only the effectiveness of our proposed stabilization strategy in improving smoothness and stability using numerical simulations. We have not applied this strategy to a real vehicle in this study, and the universality of the proposed control strategy on other models also needs to be studied. In view of the limitations, the domains of attraction, cut-in, merge, and mixed traffic (including normal vehicles, ACC vehicles, and cooperative ACC vehicles) are important topics in related studies. However, our study does not take into account these notable problems. It is hoped that these active research topics will be further investigated in future research. Moreover, an anthropomorphic and robust DSM car-following system will be developed using real vehicle test platform that can address complex traffic situations, such as congestion, in the future work.

REFERENCES

[1] J. Wang, C. Xiong, M. Lu, and K. Li, "Longitudinal driving behaviour on different roadway categories: An instrumented-vehicle experiment, data collection and case study in China," *IET Intell. Transp. Syst.*, vol. 9, no. 5, pp. 555–563, Jun. 2015.

[2] C. Miyajima, Y. Nishiwaki, K. Ozawa, T. Wakita, K. Itou, K. Takeda, and F. Itakura, "Driver modeling based on driving behavior and its evaluation in driver identification," *Proc. IEEE*, vol. 95, no. 2, pp. 427–437, Feb. 2007.

[3] L. Li, D. Wen, N.-N. Zheng, and L.-C. Shen, "Cognitive cars: A new frontier for ADAS research," *IEEE Trans. Intell. Transp. Syst.*, vol. 13, no. 1, pp. 395–407, Mar. 2012.

[4] H. Xiong and L. N. Boyle, "Drivers' adaptation to adaptive cruise control: Examination of automatic and manual braking," *IEEE Trans. Intell. Transp. Syst.*, vol. 13, no. 3, pp. 1468–1473, Sep. 2012.
[5] S. H. Hosseinnia, I. Tejado, V. Milanés, J. Villagrá, and B. M. Vinagre, "Experimental application of hybrid fractional-order adaptive cruise control at low speed," *IEEE Trans. Control Syst. Technol.*, vol. 22, no. 6, pp. 2329–2336, Nov. 2014.
[6] M. Mamouei, I. Kaparias, and G. Halikias, "A framework for user- and system-oriented optimisation of fuel efficiency and traffic flow in adaptive cruise control," *Transp. Res. C, Emerg. Technol.*, vol. 92, pp. 27–41, Jul. 2018.
[7] D. Yanakiev and I. Kanellakopoulos, "A simplified framework for string stability analysis in AHS," *IFAC Proc. Volumes*, vol. 29, no. 1, pp. 7873–7878, Jun./Jul. 1996.
[8] G. Franck, C. Vincent, and C. Francois, "A reactive multi-agent system for localization and tracking in mobile robotics," in *Proc. 16th IEEE Int. Conf. Tools Artif. Intell.*, Boca Raton, FL, USA, Nov. 2004, pp. 431–435.
[9] S.-Y. Yi and K.-T. Chong, "Impedance control for a vehicle platoon system," *Mechatronics*, vol. 15, no. 5, pp. 627–638, Jun. 2005.
[10] X.-Y. Lu, J. K. Hedrick, and M. Drew, "ACC/CACC-control design, stability and robust performance," in *Proc. Amer. Control Conf.*, Anchorage, AK, USA, vol. 6, May 2002, pp. 4327–4332.
[11] Y. Zheng, S. E. Li, J. Wang, L. Y. Wang, and K. Li, "Influence of information flow topology on closed-loop stability of vehicle platoon with rigid formation," in *Proc. 17th Int. IEEE Conf. Intell. Transp. Syst. (ITSC)*, Qingdao, China, Oct. 2014, pp. 2094–2100.
[12] V. Milanés, S. E. Shladover, J. Spring, C. Nowakowski, H. Kawazoe, and M. Nakamura, "Cooperative adaptive cruise control in real traffic situations," *IEEE Trans. Intell. Transp. Syst.*, vol. 15, no. 1, pp. 296–305, Feb. 2014.
[13] M. Treiber, A. Hennecke, and D. Helbing, "Congested traffic states in empirical observations and microscopic simulations," *Phys. Rev. E, Stat. Phys. Plasmas Fluids Relat. Interdiscip. Top.*, vol. 62, no. 2, pp. 1805–1824, Aug. 2000.
[14] V. Milanés and S. E. Shladover, "Modeling cooperative and autonomous adaptive cruise control dynamic responses using experimental data," *Transp. Res. C, Emerg. Technol.*, vol. 48, pp. 285–300, Nov. 2014.
[15] A. Kesting, M. Treiber, and D. Helbing, "Enhanced intelligent driver model to access the impact of driving strategies on traffic capacity," *Philos. Trans. Roy. Soc. A, Math., Phys. Eng. Sci.*, vol. 368, no. 1928, pp. 4585–4605, Oct. 2010.
[16] C. Lu and A. Aakre, "A new adaptive cruise control strategy and its stabilization effect on traffic flow," *Eur. Transp. Res. Rev.*, vol. 10, no. 2, pp. 49–60, Jun. 2018.
[17] B. S. Kerner, "Autonomous driving in framework of three-phase traffic theory," *Procedia Comput. Sci.*, vol. 130, pp. 785–790, Jan. 2018.
[18] B. S. Kerner, "Physics of automated driving in framework of three-phase traffic theory," *Phys. Rev. E, Stat. Phys. Plasmas Fluids Relat. Interdiscip. Top.*, vol. 97, no. 4, Apr. 2018, Art. no. 042303.
[19] G. Lu, B. Cheng, Q. Lin, and Y. Wang, "Quantitative indicator of homeostatic risk perception in car following," *Safety Sci.*, vol. 50, no. 9, pp. 1898–1905, Nov. 2012.
[20] G. Lu, B. Cheng, Y. Wang, and Q. Lin, "A car-following model based on quantified homeostatic risk perception," *Math. Problems Eng.*, vol. 2013, Nov. 2013, Art. no. 408756.
[21] K. C. Dey, L. Yan, X. Wang, Y. Wang, H. Shen, M. Chowdhury, L. Yu, C. Qiu, and V. Soundararaj, "A review of communication, driver characteristics, and controls aspects of cooperative adaptive cruise control (CACC)," *IEEE Trans. Intell. Transp. Syst.*, vol. 17, no. 2, pp. 491–509, Feb. 2016.
[22] L. Xu, L. Y. Wang, G. Yin, and H. Zhang, "Communication information structures and contents for enhanced safety of highway vehicle platoons," *IEEE Trans. Veh. Technol.*, vol. 63, no. 9, pp. 4206–4220, Nov. 2014.
[23] G. J. L. Naus, R. P. A. Vugts, J. Ploeg, M. J. G. van de Molengraft, and M. Steinbuch, "String-stable CACC design and experimental validation: A frequency-domain approach," *IEEE Trans. Veh. Technol.*, vol. 59, no. 9, pp. 4268–4279, Nov. 2010.
[24] P. Seiler, A. Pant, and K. Hedrick, "Disturbance propagation in vehicle strings," *IEEE Trans. Autom. Control*, vol. 49, no. 10, pp. 1835–1842, Oct. 2004.
[25] G. Guo and W. Yue, "Hierarchical platoon control with heterogeneous information feedback," *IET Control Theory Appl.*, vol. 5, no. 15, pp. 1766–1781, Oct. 2011.
[26] G. Guo and W. Yue, "Autonomous platoon control allowing range-limited sensors," *IEEE Trans. Veh. Technol.*, vol. 61, no. 7, pp. 2901–2912, Sep. 2012.
[27] W. Yue, G. Guo, L. Wang, and W. Wang, "Nonlinear platoon control of Arduino cars with range-limited sensors," *Int. J. Control*, vol. 88, no. 5, pp. 1037–1050, May 2015.
[28] A. Ghasemi, R. Kazemi, and S. Azadi, "Stable decentralized control of a platoon of vehicles with heterogeneous information feedback," *IEEE Trans. Veh. Technol.*, vol. 62, no. 9, pp. 4299–4308, Nov. 2013.
[29] J.-W. Kwon and D. Chwa, "Adaptive bidirectional platoon control using a coupled sliding mode control method," *IEEE Trans. Intell. Transp. Syst.*, vol. 15, no. 5, pp. 2040–2048, Oct. 2014.
[30] R. Teo, D. M. Stipanovic, and C. J. Tomlin, "Decentralized spacing control of a string of multiple vehicles over lossy datalinks," *IEEE Trans. Control Syst. Technol.*, vol. 18, no. 2, pp. 469–473, Mar. 2010.
[31] Y. Zheng, S. E. Li, J. Wang, L. Y. Wang, and K. Li, "Stability and scalability of homogeneous vehicular platoon: Study on the influence of information flow topologies," *IEEE Trans. Intell. Transp. Syst.*, vol. 17, no. 1, pp. 14–26, Jan. 2016.
[32] D. Swaroop and K. R. Rajagopal, "A review of constant time headway policy for automatic vehicle following," in *Proc. IEEE Intell. Transp. Syst. (ITSC)*, Oakland, CA, USA, Aug. 2001, pp. 65–69.
[33] X. Huppe, J. de Lafontaine, M. Beauregard, and F. Michaud, "Guidance and control of a platoon of vehicles adapted to changing environment conditions," in *Proc. Conf. IEEE Int. Conf. Syst., Man Cybern. Conf. Theme-Syst. Secur. Assurance*, Washington, DC, USA, vol. 4, Oct. 2003, pp. 3091–3096.
[34] D. Yanakiev and I. Kanellakopoulos, "Variable time headway for string stability of automated heavy-duty vehicles," in *Proc. 34th IEEE Conf. Decis. Control*, Orleans, LA, USA, vol. 4, Dec. 1995, pp. 4077–4081.
[35] A. Ghasemi, R. Kazemi, and S. Azadi, "Exact stability of a platoon of vehicles by considering time delay and lag," *J. Mech. Sci. Technol.*, vol. 29, no. 2, pp. 799–805, Feb. 2015.
[36] M. di Bernardo, P. Falcone, A. Salvi, and S. Santini, "Design, analysis, and experimental validation of a distributed protocol for platooning in the presence of time-varying heterogeneous delays," *IEEE Trans. Control Syst. Technol.*, vol. 24, no. 2, pp. 413–427, Mar. 2016.
[37] X. Guo, J. Wang, F. Liao, and R. S. H. Teo, "Distributed adaptive integrated-sliding-mode controller synthesis for string stability of vehicle platoons," *IEEE Trans. Intell. Transp. Syst.*, vol. 17, no. 9, pp. 2419–2429, Sep. 2016.
[38] R. Sipahi, F. M. Atay, and S.-I. Niculescu, "Stability analysis of a constant time-headway driving strategy with driver memory effects modeled by distributed delays," *IFAC-PapersOnLine*, vol. 48, no. 12, pp. 376–381, Jan. 2015.
[39] S. Öncü, J. Ploeg, N. van de Wouw, and H. Nijmeijer, "Cooperative adaptive cruise control: Network-aware analysis of string stability," *IEEE Trans. Intell. Transp. Syst.*, vol. 15, no. 4, pp. 1527–1537, Aug. 2014.
[40] D. Swaroop, J. K. Hedrick, C. C. Chien, and P. Ioannou, "A comparision of spacing and headway control laws for automatically controlled vehicles," *Vehicle Syst. Dyn.*, vol. 23, no. 1, pp. 597–625, Jan. 1994.
[41] A. Ali, G. Garcia, and P. Martinet, "The flatbed platoon towing model for safe and dense platooning on highways," *IEEE Intell. Transp. Syst. Mag.*, vol. 7, no. 1, pp. 58–68, Spring 2015.
[42] X. Guo, J. Wang, F. Liao, R. Teo, and H. Teo, "Distributed adaptive sliding mode control strategy for vehicle-following systems with nonlinear acceleration uncertainties," *IEEE Trans. Veh. Technol.*, vol. 66, no. 2, pp. 981–991, Feb. 2017.
[43] L. Li, G. Lu, Y. Wang, and D. Tian, "A rear-end collision avoidance system of connected vehicles," in *Proc. 17th Int. IEEE Conf. Intell. Transp. Syst. (ITSC)*, Qingdao, China, Oct. 2014, pp. 63–68.
[44] W. Reilly, *Highway Capacity Manual 2000*. Washington, DC, USA: TRB, National Research Counci, 1997.
[45] M. Treiber and A. Kesting, *Traffic Flow Dynamics: Data, Models and Simulation*. Berlin, Germany: Springer-Verlag, 2013.
[46] P. G. Gipps, "A behavioural car-following model for computer simulation," *Transp. Res. B, Methodol.*, vol. 15, no. 2, pp. 105–111, Apr. 1981.
[47] D. Vangi and A. Virga, "Evaluation of emergency braking deceleration for accident reconstruction," *Vehicle Syst. Dyn.*, vol. 45, no. 10, pp. 895–910, Aug. 2007.
[48] E. Sokolovskij, "Experimental investigation of the braking process of automobiles," *Transport*, vol. 20, no. 3, pp. 91–95, Jan. 2005.

[49] J. Zhang, Y. Wang, and G. Lu, "Extended desired safety margin car-following model that considers variation of historical perceived risk and acceptable risk," *Transp. Res. Rec., J. Transp. Res. Board*, vol. 2672, no. 20, pp. 86–97, Dec. 2018.
[50] P. Wagner, "Analyzing fluctuations in car-following," *Transp. Res. B, Methodol.*, vol. 46, no. 10, pp. 1384–1392, Dec. 2012.
[51] R. Jiang, M.-B. Hu, H. M. Zhang, Z.-Y. Gao, B. Jia, Q.-S. Wu, B. Wang, and M. Yang, "Traffic experiment reveals the nature of car-following," *PLoS ONE*, vol. 9, no. 4, Apr. 2014, Art. no. e94351.
[52] Y. Wang, J. Zhang, and G. Lu, "Influence of driving behaviors on the stability in car following," *IEEE Trans. Intell. Transp. Syst.*, vol. 20, no. 3, pp. 1081–1098, Mar. 2019.
[53] N. Sun, Y. Fang, and H. Chen, "A new antiswing control method for underactuated cranes with unmodeled uncertainties: Theoretical design and hardware experiments," *IEEE Trans. Ind. Electron.*, vol. 62, no. 1, pp. 453–465, Jan. 2015.
[54] J.-D. Lee and R.-Y. Duan, "Cascade modeling and intelligent control design for an electromagnetic guiding system," *IEEE/ASME Trans. Mechatronics*, vol. 16, no. 3, pp. 470–479, Jun. 2011.
[55] A. Pisano, A. Davila, L. Fridman, and E. Usai, "Cascade control of PM-DC drives via second-order sliding mode technique," in *Proc. Int. Workshop Variable Struct. Syst.*, Antalya, Turkey, Jun. 2008, pp. 268–273.
[56] B. Li and W. Jiang, "Chaos optimization method and its application," *Control Theory Appl.*, vol. 14, no. 4, pp. 613–615, Aug. 1997.
[57] M. Mulder, D. A. Abbink, M. M. van Paassen, and M. Mulder, "Design of a haptic gas pedal for active car-following support," *IEEE Trans. Intell. Transp. Syst.*, vol. 12, no. 1, pp. 268–279, Mar. 2011.

MINGFEI MU was born in Shandong, China, in 1990. He received the B.S. degree from the Central South University, Changsha, China, in 2012, and the Ph.D. degree from Beihang University, Beijing, China, in 2019. He is currently an Assistant Professor with Shandong University of Science and Technology, Qingdao, China. His research interests include transportation optimization and green-car technology.

JUNJIE ZHANG received the Ph.D. degree from the School of Transportation Science and Engineering, Beihang University, Beijing, China, in 2019. He received a Postdoctoral Scholar with the School of Electronic and Information Engineering, Beihang University, in 2021. He is currently an Associate Professor with Hefei Innovation Research Institute, Beihang University, Hefei, China. His research interests include traffic flow theory, travel behavior analysis and modeling, and vehicle-to-vehicle cooperative control.

CHANGMIAO WANG was born in Shandong, China, in 1989. He received the Ph.D. degree in pattern recognition and intelligent systems from the University of Chinese Academy of Sciences, Beijing, in 2018. From 2018 to 2020, he acted as a Postdoctoral Fellow with the School of Science and Engineering, The Chinese University of Hong Kong, Shenzhen, and the University of Science and Technology of China. He is currently an Assistant Professor with Shenzhen Research Institute of Big Data. His research interests include medical vision, medical image analysis, computer vision, deep learning, and reinforcement learning.

JUN ZHANG was born in Anhui, China, in 1981. He received the M.S. and Ph.D. degrees in signal and information processing from Hefei Electronic Engineering Institute, Hefei, China, in 2005 and 2008, respectively. He is currently working as a Postdoctoral Scholar with Hefei Innovation Research Institute, Beihang University. His research interests include LiDAR SLAM and localization based on multi-sensor fusion.

CAN YANG received the M.S. degree from Beihang University, Beijing, China, in 2015. She is currently an Engineer with the Hefei Innovation Research Institute, Beihang University, Hefei, China. Her research interests include traffic flow operation and control and transportation behavior modeling.